



Hydrogen concentrations on C-class asteroids derived from remote sensing

A. S. RIVKIN,^{1*} J. K. DAVIES,² J. R. JOHNSON,³ S. L. ELLISON,^{4†}
D. E. TRILLING,⁵ R. H. BROWN,⁶ and L. A. LEBOSKY⁶

¹Massachusetts Institute of Technology, 77 Massachusetts Avenue, Cambridge, Massachusetts 02139, USA

²UK Astronomy Technology Center, Royal Observatory Edinburgh, Edinburgh EH9 3HJ, UK

³United States Geological Survey Astrogeology Team, Flagstaff, Arizona 86001, USA

⁴Departamento de Astronomia, P. Universidad Católica de Chile, Casilla 306, Santiago 22, and
European Southern Observatory, Casilla 19001, Santiago 19, Chile

⁵University of Pennsylvania, Department of Physics and Astronomy, David Rittenhouse Laboratory,
209 S. 33rd St., Philadelphia, Pennsylvania 19104, USA

⁶Department of Planetary Sciences, University of Arizona, Tucson, Arizona 85721, USA

[†]Present address: University of Victoria, Elliott Building, 3800 Finnerty Rd, Victoria, BC, V8P 1A1, Canada

*Corresponding author. E-mail: asrivkin@mit.edu

(Received 21 February 2003; revision accepted 15 August 2003)

Abstract—We present spectroscopic observations of 16 asteroids from 1.9–3.6 μm collected from the United Kingdom Infrared Telescope (UKIRT) from 1996–2000. Of these 16 asteroids, 11 show some evidence of a 3 μm hydrated mineral absorption feature greater than 2σ at 2.9 μm . Using relations first recognized for carbonaceous chondrite powders by Miyamoto and Zolensky (1994) and Sato et al. (1997), we have determined the hydrogen to silicon ratio for these asteroids and calculated their equivalent water contents, assuming all the hydrogen was in water. The asteroids split into 2 groups, roughly defined as equivalent water contents greater than $\sim 7\%$ (8 asteroids, all with 3 μm band depths greater than $\sim 20\%$) and less than $\sim 3\%$ for the remaining 8 asteroids. This latter group includes some asteroids for which a weak but statistically significant 3 μm band of non-zero depth exists. The G-class asteroids in the survey have higher water contents, consistent with CM chondrites. This strengthens the connection between CM chondrites and G asteroids that was proposed by Burbine (1998). We find that the 0.7 μm and 3 μm band depths are correlated for the population of target objects.

BACKGROUND AND PREVIOUS WORK

The presence of water- and hydroxyl-bearing minerals (hereafter called “hydrated minerals”) in meteorites and asteroids is long-established (DuFresne and Anders 1962; Lebofsky 1978; Lebofsky 1980). Given the potential importance of asteroid impacts as a source of water to the early Earth (Delsemme 2000; Morbidelli et al. 2000) and the possible use of asteroids for resource utilization purposes (Lewis et al. 1993), quantifying the amount of water present in the asteroid population is critical. We present a means of making a quantitative assessment of the H/Si ratio on C-class asteroid surfaces using remote sensing (Results section). First, however, we review both asteroid taxonomy as is appropriate to this work and previous studies of hydrated minerals on asteroids (C-Class Asteroids: Taxonomies and Hydrated Minerals on C-Class Asteroids subsections). We describe our observations and data reduction in the Observations and Thermal Flux Corrections sections. We

consider implications of the data and calculated H/Si ratios in the Discussion section. Finally, a discussion of future work can be found in the Future Work section.

C-Class Asteroids: Taxonomies

The spectral taxonomy for asteroids of Tholen (1984) defined a large C taxon, subdivided into “C,” “B,” “F,” and “G” subclasses. These have been interpreted as related to each other via differing amounts of alteration of a common progenitor material, probably related to carbonaceous chondrite meteorites (Gaffey et al. 1989). In this taxonomy, 1 Ceres is a G-class asteroid, and 2 Pallas is a B-class asteroid.

The taxonomy of Bus and Binzel (2002) includes much of the Tholen (1984) terminology, wherever possible, to maintain consistency. They have a large “C complex” with a variety of subclasses (B, C, Cb, Cg, Ch, Cgh). In this taxonomy, for comparison, 1 Ceres is a C-class asteroid, while 2 Pallas remains a B-class asteroid.

All of the asteroids included in this work have been classified in 1 of the C subclasses by both Tholen (1984) and Bus and Binzel (2002), with 2 exceptions: 375 Ursula was classified as C-class by Tholen but Xc by Bus and Binzel. The Xc-class is “next door” to the C complex in principal component space, however. The other exception is somewhat more serious: 980 Anacostia was classified as SU by Tholen and as L by Bus and Binzel. It is included here because it may have some affinity to the CV/CO meteorites (Burbine et al. 1992) and, thus, belongs in a discussion of carbonaceous chondrite analogues. The spectral classifications for the target asteroids in both the Bus and Binzel (2002) and Tholen (1984) taxonomies are found in Table 1.

Hydrated Minerals on C-Class Asteroids

Hydrated minerals give rise to absorptions throughout the infrared spectral region. The strongest absorptions occur near 3 μm , where features due to OH vibrational fundamentals ($\sim 2.75 \mu\text{m}$) as well as the first overtone of H_2O ($\sim 3.1 \mu\text{m}$) are found. The result is a broad absorption band stretching from 2.7–3.5 μm or beyond, which is generally referred to as the “3 μm band.” Because the OH fundamental has its band minimum at a wavelength that is difficult to observe from the ground for objects of asteroidal brightness, the band depth for the 3 μm band on asteroids must be measured at a different wavelength. In this work, we measure the band depth at 2 wavelengths: 2.9 and 3.2 μm .

Lebofsky et al. (1981) concluded that 1 Ceres had a surface dominated by minerals similar to terrestrial montmorillonites, based on its 3 μm band shape. King et al. (1992) instead suggested ammoniated phyllosilicates as analogues for Ceres’ surface. Larson et al. (1983) argued that 2 Pallas was roughly analogous to CI/CM meteorites based on a qualitative list of common spectral characteristics. A

quantitative investigation of a larger population has not been made, however.

Feierberg et al. (1985) obtained 3 μm spectra of 14 C-class asteroids, finding correlations between band depth and UV absorption strength shortward of 0.4 μm and suggesting that the C-class may consist of fragments of anhydrous, CV/CO₃-like cores and hydrated CI1- or CM2-like mantles. Jones et al. (1990) increased the sample size to 32 C-class asteroids, finding 66% of them to have hydrated silicate surfaces and that the hydrated mineral abundances of C-class asteroids decline gradually from 2.5–3.5 AU. The work of Jones et al. (1990) and Feierberg et al. (1985) allowed the first reckoning of the hydration state of the C-class as a whole. However, the instruments available in the 1980s were only able to provide a binary “yes/no” to hydration state rather than detailed, quantitative band depths and shapes for a large number of objects.

More recently, an absorption feature near 0.7 μm has been correlated with the 3 μm water of the hydration feature by Vilas (1994) and Howell et al. (2001). Hiroi et al. (1996) used the relative strengths of the 0.7 μm and 3 μm bands to conclude that the C asteroids suffered thermal metamorphism as discussed below. The taxonomy of Bus and Binzel (2002) appends an “h” when the 0.7 μm band is found in C-class or C-subclass asteroids. Again, this serves simply to inform that hydrated minerals do (or do not) exist rather than quantitatively interpreting them. Indeed, at this point, the correlation between the depth of the 0.7 μm band and the amount of hydrated minerals is still under investigation (Howell et al. 2001).

OBSERVATIONS

These data were taken using CGS4, a cooled grating array spectrometer (Mountain et al. 1990), on the United Kingdom Infrared Telescope (UKIRT) from 1996–2000. This

Table 1. Asteroids observed at UKIRT. Taxonomic classifications in both the Bus and Binzel and Tholen schemes are included, as well as the observers present at the telescope.

Date	Asteroid	Tholen	Bus	Standard	Observers
02/04/1996	2 Pallas	B	B	BS 5384	Rivkin, Davies, Johnson
	13 Egeria	G	Ch	BS 1164	
	51 Nemausa	CU	Ch	SAO 11691	
07/10/1997	1 Ceres	G	C	SAO 165572	Rivkin, Davies, Ellison
	19 Fortuna	G	Ch	SAO 146142	
	106 Dione	G	Cgh	SAO 188048	
08/11/1998	185 Eunike	C	C	BS 9107	Rivkin, Davies
	375 Ursula	C	Xc	BS 9107	
08/12/1998	980 Anacostia	SU	L	BS 6836	
	521 Brixia	C	Ch	BS 88	
08/13/1998	59 Elpis	CP	B	BS 6998	
	238 Hypatia	C	Ch	BS 8314	
01/28/2000	45 Eugenia	FC	C	BS 4533	Rivkin, Davies, Trilling
01/29/2000	52 Europa	CF	C	SAO 119398	
10/02/2000	324 Bamberg	CP	–	SAO 56391	Rivkin, Davies
10/04/2000	704 Interamnia	F	B	SAO 161071	

spectrometer covers $0.67 \mu\text{m}$ per grating setting, so 3 settings (center wavelengths at 2.20 , 2.76 , and $3.23 \mu\text{m}$) were used to cover the wavelength region of interest with sufficient overlap to allow for proper normalization. This resulted in coverage from 1.9 – $3.6 \mu\text{m}$. The grating ranges, as well as a plot of the atmospheric transmission, can be found in Fig. 1. Because the middle grating covers 2.45 – $3.10 \mu\text{m}$ simultaneously, including regions both longward and shortward of the spectral region unobservable due to telluric water, scaling of the $\lambda < 2.5 \mu\text{m}$ and $\lambda > 2.9 \mu\text{m}$ data to one another can be done in a straightforward manner. Some of the objects only had data taken through the 2 longer-wavelength gratings, resulting in 2.45 – $3.6 \mu\text{m}$ spectra.

Standard star observations were contiguous with asteroid observations. Each asteroid had a standard star chosen to be of roughly solar type (and main sequence when possible) and to minimize airmass differences. The standard stars used for each asteroid are also shown in Table 1. Because the K – L colors for main sequence stars differ from solar by only 1–2% from F2 all the way to K1 (Koornneef 1983) and all of the standard stars fall within that classification range, no further correction to solar colors was performed. For comparison, the sun is a G2 star, which is in the middle of that stellar classification range.

To decrease observational uncertainties, the data, which

originally had a spectral resolution of $\lambda/\Delta\lambda = 400$, were binned by a factor of 24. The science goals of searching for broad hydrated mineral absorption features and determining continuum levels in the 2.5 – $3.5 \mu\text{m}$ region were easily met at this resolution. The binning was done simply by dividing the data into 64 regions of 24 pixels each and determining the new average and standard deviation for each 24-pixel region.

THERMAL FLUX CORRECTIONS

Longward of roughly $3 \mu\text{m}$, the signal received from bodies in the asteroid belt contains both thermal and reflected components. Therefore, thermal corrections were calculated using the Standard Thermal Model (STM), described in Lebofsky et al. (1989), to determine the true reflectance spectrum. Models with beaming parameters (η) with values of 0.756, 0.85, 0.9, and 1.0 were calculated for each object. Plus, an additional model with $\eta = 0.78$ was calculated for 324 Bamberga. This range of model values for η roughly matches the values seen among main-belt asteroids. Larger values for η result in models with less predicted thermal flux. While the uncertainty in the thermal correction increases with wavelength, it is quite small at the wavelengths of greatest interest near $3 \mu\text{m}$. Furthermore, because the thermal

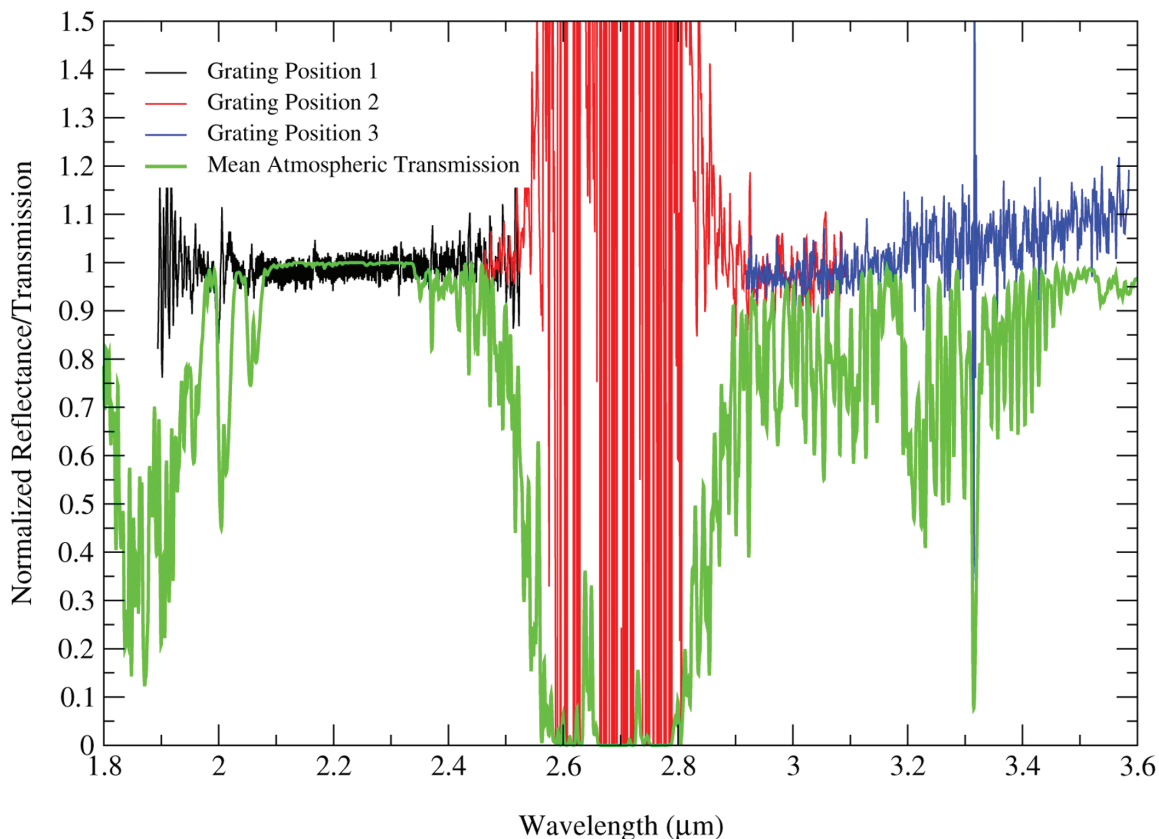


Fig. 1. Grating positions and atmospheric transmission: The spectrum shown here (980 Anacostia/BS 6836) is composed of data taken in 3 grating positions, shown in black, red, and blue. The overlap enables us to create a single, continuous spectrum. Atmospheric transmission varies from 0–1 over the range of the spectrum.

correction increases monotonically with wavelength throughout this spectral region (and well beyond), one cannot create a spurious local minimum by applying a thermal correction. The effect of using too small a value for η is to overestimate the contribution of thermal flux and create a spectrum that decreases with increasing wavelength, which is not seen in meteorite samples. This effect is obvious and thus avoidable. The effect of using too large a value for η would conversely lead to a spectrum that increases with increasing wavelength. This case is somewhat more difficult to diagnose, since some objects have reflectances that truly do increase with increasing wavelength. An example of the effect of changing η upon thermal corrections is shown in Fig. 2.

The value of η used for each asteroid was chosen by inspection of the resulting spectrum, with the selected values (as well as values for albedo and diameter from Tedesco et al. [1992], Millis et al. [1984], and Storrs et al. [1999]) shown in Table 2. These values were selected such that the behavior at 3.6 μm matched a continuum extrapolated from the 2.4 μm region. Where 2 thermal corrections seemed equally well-suited, the one with a larger η was selected because that used the smaller correction, at the potential cost of underestimating

the band depth at 3.2 μm . The effect this had on the resulting H/Si ratio is discussed in the Results for Asteroids section. The values of η that were chosen for the various asteroids spanned the entire range from 0.756 to 1.0. This is not wholly unexpected, since the beaming parameter is an abstraction of surface roughness, thermal inertia, and other properties, which are difficult to model explicitly, and the range of beaming parameters among asteroids is seen to vary from 0.756 for Ceres and Pallas (Lebofsky et al. 1986) to 1.2 for near-Earth asteroids (Harris 1998). For some of our target asteroids (2 Pallas, 13 Egeria; see Fig. 3), the long-wavelength continuum ($\sim 3.6 \mu\text{m}$) falls below the level of the short-wavelength continuum ($\sim 2.4 \mu\text{m}$). This behavior is also seen in hydrated mineral spectra (Salisbury et al. 1991) and so, again, is not unexpected.

RESULTS

3- μm Band Depths and Band Shapes

Figure 3 shows the thermally-corrected spectra of the target asteroids. The band depths at 2.9 and 3.2 μm (calculated as $1 - R_\lambda/R_{2.5}$) are shown in Table 3. Eleven of them show

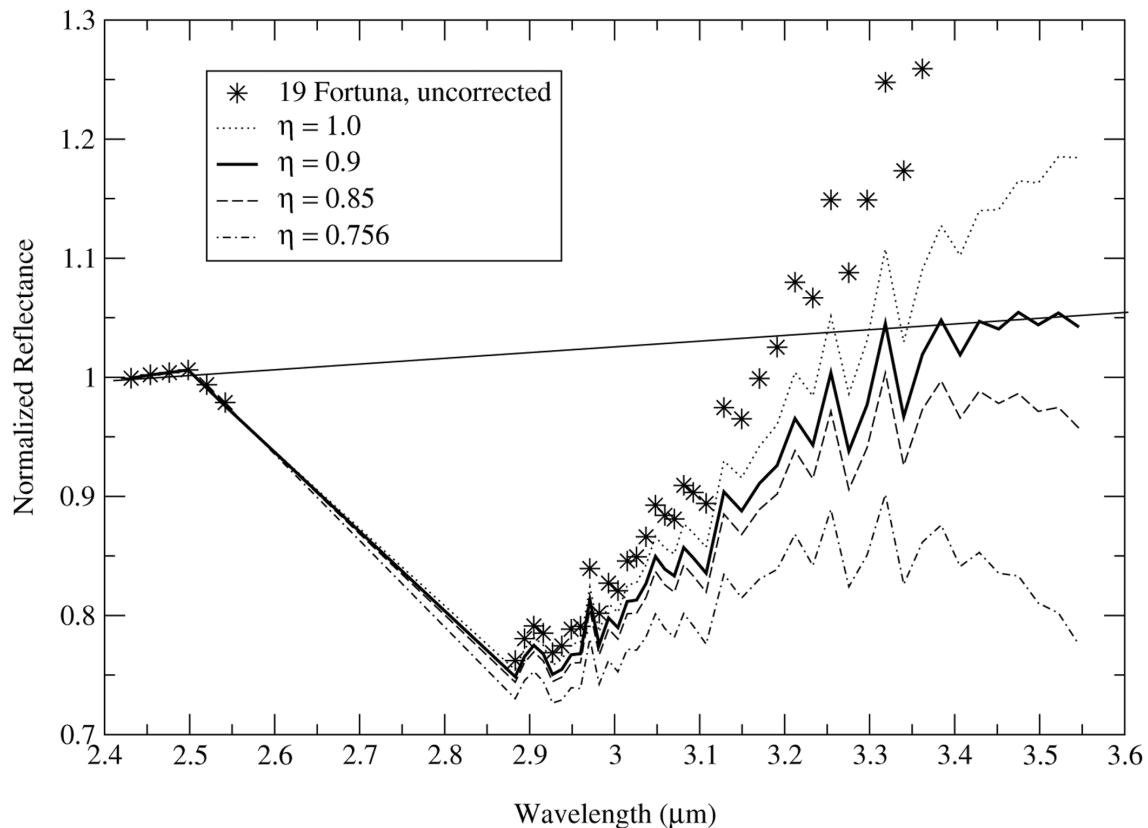


Fig. 2. Effect of thermal corrections. The spectrum of 19 Fortuna, uncorrected (symbols) and corrected, using thermal models with differing values of the beaming parameter (η) is shown. A value of (η) that is too small results in overcorrection of the data and a spectrum that dips with increasing wavelength starting $\sim 3.4 \mu\text{m}$. The chosen model (heavy solid line) results in a continuum near 3.5 μm of a similar slope to the continuum near 2.4 μm (light solid line).

Table 2. The diameters, albedos, and thermal parameters (η) used in the thermal models for target asteroids. The diameters and albedos are from IRAS measurements, except for 19 Fortuna and 375 Ursula.

Asteroid	Diameter	Albedo	η
1 Ceres	848 km	0.113	0.756
2 Pallas	498 km	0.159	0.756
13 Egeria	208 km	0.083	0.90
19 Fortuna ^a	225 km	0.05b	0.90
45 Eugenia	215 km	0.040	0.90
51 Nemausa	148 km	0.093	0.90
52 Europa	303 km	0.058	0.85
59 Elpis	165 km	0.044	0.85
106 Dione	147 km	0.089	0.85
185 Eunike	158 km	0.064	0.85
238 Hypatia	149 km	0.043	1.00
324 Bamberga	229 km	0.063	0.78
375 Ursula ^b	216 km	0.032	0.90
521 Brixia	116 km	0.063	0.756
704 Interamnia	317 km	0.074	0.85
980 Anacostia	86 km	0.172	1.00

^aThe diameter of 19 Fortuna was taken from HST observations by Storrs et al. (1999) with its albedo derived from that diameter and its published absolute magnitude.

^bMillis et al. (1984) found the diameter of 375 Ursula from an occultation and derived its albedo.

evidence of a 3 μm absorption band with $>2\sigma$ detection at 2.9 μm . Four of the asteroids have no observable feature within 1σ . Asteroid 704 Interamnia has an apparent 2.9 μm band at $9.3 \pm 5.9\%$, or roughly 1.5σ . This ratio of hydrated to anhydrous C-class asteroids ($\sim 2:1$) has been seen in a number of other works (Jones et al. 1990; Vilas 1994), but we caution the reader that the sample of targets in this work was chosen partially on the basis of previous work and so is not unbiased. Of the 7 new objects presented here, 3 show no 2.9 μm feature greater than 1σ , while 4 show 2σ or greater features. Though a small sample, this, too, is in rough agreement with what would be expected. In general, the band shapes appear similar to each other where present, with a presumed band minimum in the spectral region obscured by the atmosphere and with reflectance increasing roughly linearly with wavelength beyond that. Two asteroids, 1 Ceres and 375 Ursula, have 3 μm band shapes that are more rounded and do not fit this description. None of the target asteroids have an apparent “inverse” feature, which would be expected on some of the asteroids if the 3 μm feature were due to incomplete atmospheric correction. In no case does a negative band depth greater than 1σ at 2.9 μm exist, where imperfect atmospheric correction would have a large effect. Some of the values of band depth at 3.2 μm shown in Table 3 suggest a negative feature. However, these can all be explained by 2 factors: first, the decision to choose the smaller thermal correction when presented with 2 equally good thermal models can lead to a reflectance at 3.2 μm that is higher than it “should” be; second, because the values for band depth in Table 3 assume a flat

Table 3. 2.9 and 3.2 μm band depths for target asteroids. These were calculated as $(1 - R_\lambda/R_{2.5})$, with thermal flux removed. The 3.2 μm band depth is not near the band minimum and is included to allow rederivation of H/Si ratios. The uncertainty for the band depths is the square root of the sum of the squares of the uncertainties at 2.5 μm and either 2.9 or 3.2 μm .

Asteroid	2.9 μm band depth	\pm	3.2 μm band depth	\pm
1 Ceres	20.4%	1.3%	19.0%	3.3%
2 Pallas	21.8	1.6	7.2	1.5
13 Egeria	30.3	2.6	12.6	4.8
19 Fortuna	23.8	2.2	7.5	5.4
45 Eugenia	0.4	2.6	-13.9	4.2
51 Nemausa	38.8	2.2	11.9	2.2
52 Europa	6.2	2.0	1.7	3.8
59 Elpis	-1.8	5.9	-5.1	5.9
106 Dione	40.2	8.4	19.6	29.6
185 Eunike	5.3	2.0	3.4	3.6
238 Hypatia	19.5	2.9	8.7	6.9
324 Bamberga	-1.9	2.0	-5.3	4.9
375 Ursula	3.6	1.8	4.2	3.3
521 Brixia	24.8	4.0	3.2	5.8
704 Interamnia	9.3	5.9	1.8	5.6
980 Anacostia	-0.2	4.4	0.6	2.5

continuum beyond 2.5 μm , an object with a sloping continuum and little or no 3 μm band would have a reflectance at 3.2 μm higher than at 2.5 μm and a negative band depth relative to the assumed flat continuum.

The 3 μm band shapes can be roughly quantified using a plot first introduced by Sato et al. (1997). Figure 4 shows the 2.9 $\mu\text{m}/2.5 \mu\text{m}$ reflectance ratio versus the 3.2 $\mu\text{m}/2.5 \mu\text{m}$ reflectance ratio for a number of carbonaceous chondrite spectra, as well as for the target asteroids. The meteorite data come from Hiroi et al. (1996) and Jones (1988). The meteorite data trend along a line on such a plot. The majority of target asteroids also fall along this linear trend. However, Ceres and Ursula are off the trend because of their unusual spectra in the 3 μm region. On this plot, anhydrous meteorites and asteroids fall near (1, 1) or to the upper right of that point. The fact that the asteroids fall along the meteorite trend is consistent with their surfaces being similar in hydrated mineral composition.

Determining the Hydrogen to Silicon Ratio

Recent work in the field of meteorite studies has shown that it is possible to estimate the amount of water in an asteroidal regolith. Miyamoto and Zolensky (1994) showed that the integrated intensity of the 3 μm absorption band is correlated with the hydrogen to silicon ratio in carbonaceous chondrite powders. Later work by Sato et al. (1997) showed that the integrated intensity of the 3 μm band in carbonaceous chondrite powders is related to the ratio of the 2.9 μm (as well as the 3.2 μm) reflectance to 2.5 μm reflectance. We again

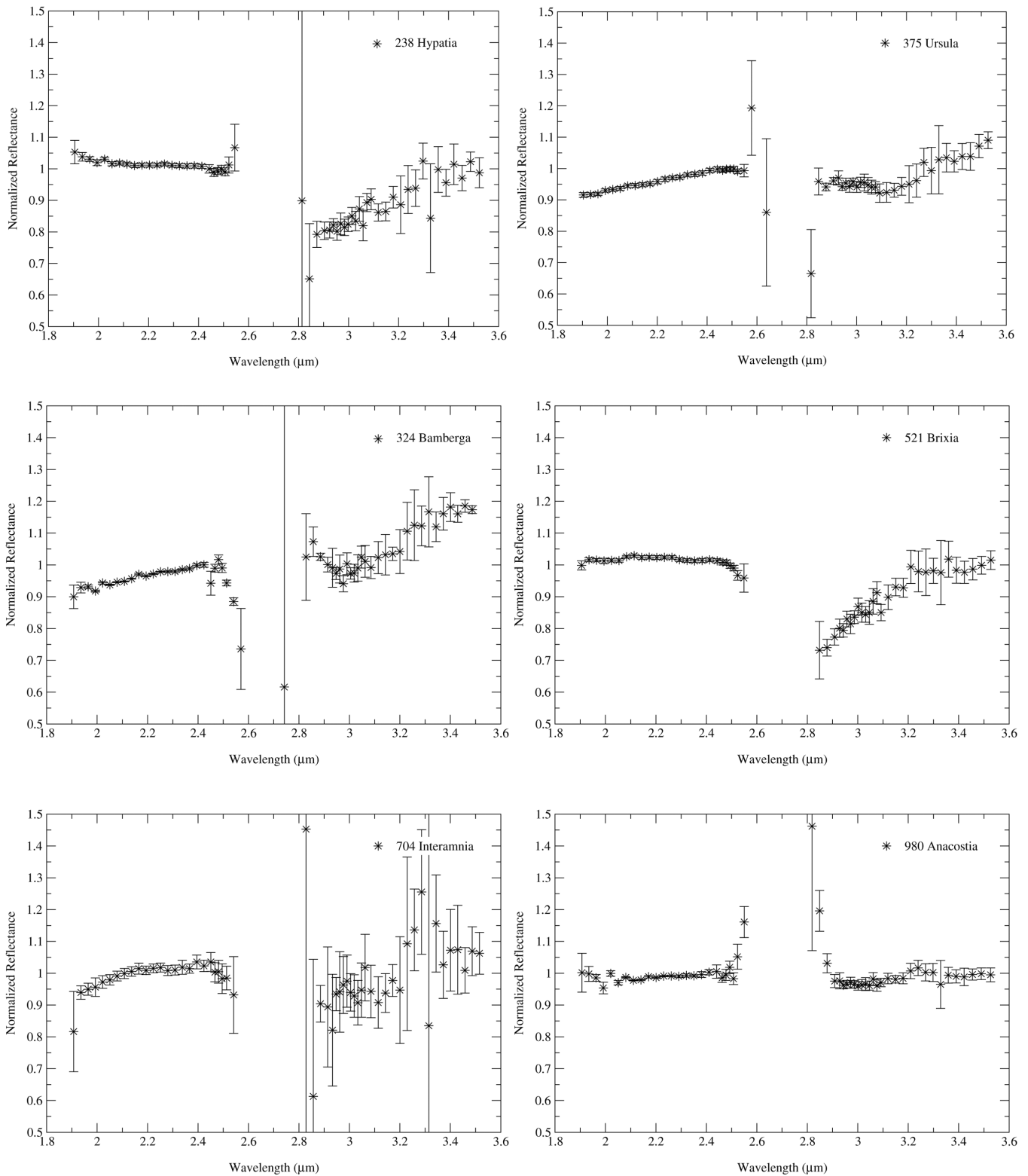


Fig. 3. Thermally corrected spectra of the target asteroids, 1996–2000.

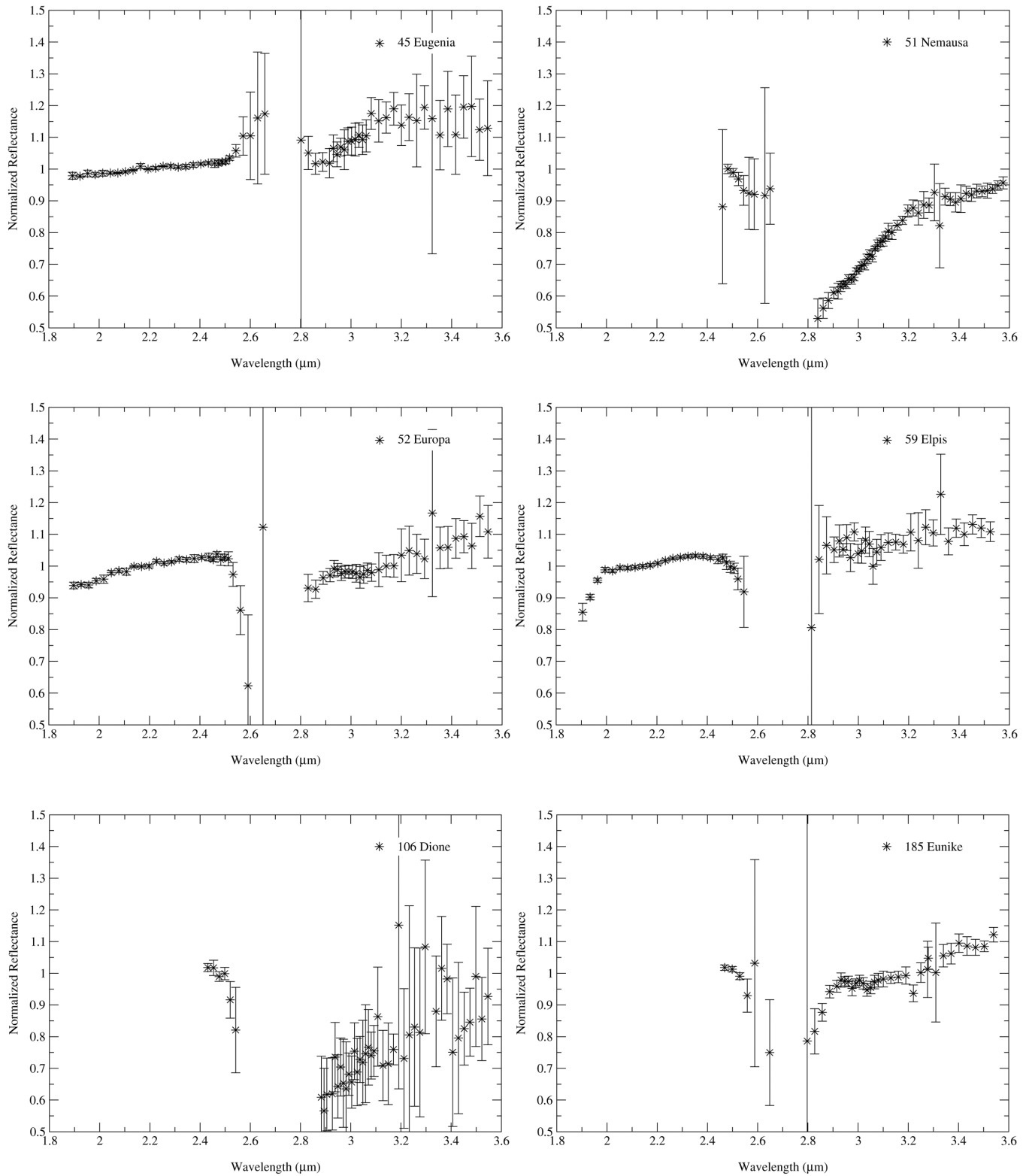


Fig. 3. Thermally corrected spectra of the target asteroids, 1996–2000.

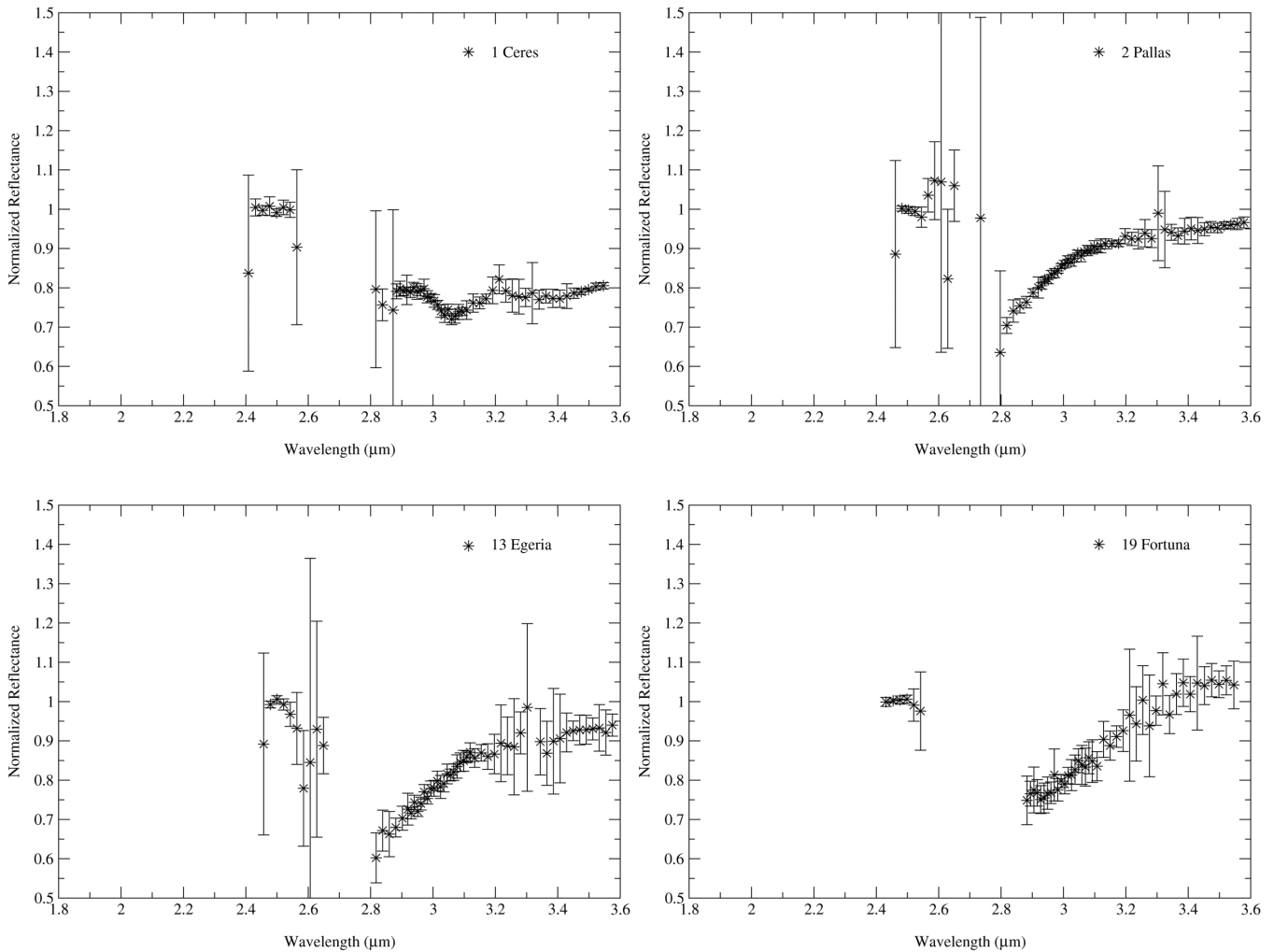


Fig. 3. Thermally corrected spectra of the target asteroids, 1996–2000.

stress that these ratios do not represent different absorption features but band depths for the broad 3 μm band measured at 2 different wavelengths. Put together, one can determine the H/Si ratio remotely assuming the target surface is analogous to the powders used in the studies.

We performed a linear least-squares fit to the Miyamoto and Zolensky (1994) data, digitized from their Fig. 4, to obtain an analytical expression for the H/Si ratio as a function of integrated intensity. Similarly, we fit both the 2.9 and 3.2 μm reflectance ratios as a function of integrated intensity, following Sato et al. (1997). The fits to these data are shown in Figs. 5 and 6. We then combined these 2 functions to get the H/Si ratio as a function of the reflectance ratios:

$$\text{H/Si} = 7.38 - 7.29 \times R_{2.9}/R_{2.5} \quad (1)$$

$$\text{H/Si} = 11.85 - 11.07 \times R_{3.2}/R_{2.5} \quad (2)$$

We note that these relations are experimentally-based rather than derived from first principles. Furthermore, they will only hold for surfaces that are analogous to carbonaceous chondrite

powders. Finally, the nature of reflectance spectroscopy is such that only the surface of the body is sensed (technically speaking, only the top $\sim 10 \mu\text{m}$ or so, though mixing within the regolith should homogenize at least the top several cm, using the lunar regolith as a guide [Hörz et al. 1991]). Thus, the H/Si ratio determined for the surface of an asteroid may be different from the bulk H/Si ratio for the entire body. Note further that a band depth of zero does not mean that $R_{2.9}/R_{2.5}$ or $R_{3.2}/R_{2.5}$ is equal to 1 because the continuum was not removed from the original Sato et al. (1997) data. A body with no hydrogen would be calculated to have a $R_{2.9}/R_{2.5}$ value of 1.01 and a $R_{3.2}/R_{2.5}$ value of 1.07 using these equations.

Equations 1 and 2 were used to calculate the H/Si ratios and equivalent water contents for the target asteroids and control meteorites in Figs. 7 and 8.

Equivalent Water Contents

To estimate water contents from the H/Si ratio, a value for bulk Si concentration is needed. This is provided for

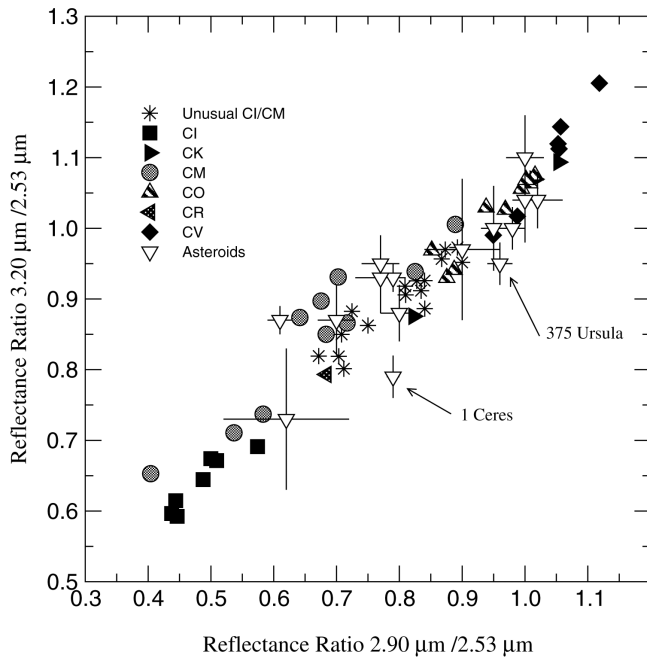


Fig. 4. On a diagram of 3.2/2.5 μm reflectance versus 2.9/2.5 μm reflectance, the carbonaceous chondrites follow a linear trend, first shown by Sato et al. (1997). The asteroids in this work also follow the same trend, except for 1 Ceres and 375 Ursula. Other than those 2, the other asteroids all have spectra consistent with carbonaceous chondrites. The meteorite data in this plot are from Hiroi et al. (1996) and Jones (1988).

various meteorite classes in Jarosewich (1990). Given this number, the weight percentage of H can be determined. To maintain consistency with the tables of modal analyses given in geochemical works, the hydrogen is all assumed to be in H_2O , though it is almost certainly in hydroxyl (OH) instead. For this reason, we refer to it as “equivalent water content.” However, the geological interpretation is the same whether the hydrogen is found in OH or H_2O : the hydrogen-bearing minerals were formed through aqueous alteration on the parent body (or perhaps through nebular processes which created phyllosilicates) and are now visible on the surface (see Zolensky et al. [1997] for a recent discussion of meteoritical interpretations of water-bearing minerals). Other hydrogen carriers such as organic carbon compounds are not likely to be found in amounts comparable to clays on asteroid surfaces. If an asteroidal surface is very organic-rich but OH-poor, it would appear to have a low H/Si ratio by this technique. However, such an asteroidal spectrum would look quite different from those presented here and would certainly be flagged for further study. Searches for organic materials on asteroids in this spectral region have, so far, yielded negative results (Cruikshank et al. 2002; Emery 2002).

We used a bulk SiO_2 concentration of 30% for the asteroids, which is the CM average reported in Jarosewich (1990). Given this, we can determine the equivalent water content of the target asteroids from their reflectance spectra:

$$\text{Equiv. water} = 0.5 \times \text{H/Si} \times \text{wt. frac. SiO}_2 \times \text{atomic wt. H}_2\text{O/atomic wt. SiO}_2 \quad (3)$$

The factor of 0.5 is necessary to account for the fact that 2 hydrogens go into water, rather than just 1. This is why the explicit assumption that the hydrogen is in water rather than hydroxyl is necessary. The equivalent water contents for the target asteroids are shown in Fig. 9. These water contents are shown using the 2.9 μm reflectance ratio only (see below). An estimate of the uncertainties involved in the calculations is provided in the Test on Meteorites subsection.

Because the H/Si ratio does not contain any assumptions about the silicate mineralogy of the target asteroids, it is preferred for quantitatively determining good analogues. However, the water contents are also included here since they potentially provide a good qualitative means of comparison with a wide range of materials, and because the weight fraction of water is a more familiar quantity than H/Si ratio.

Test on Meteorites

We tested the accuracy of Equations 1–3 by determining the water contents for 6 meteorites for which both published 3 μm spectra and laboratory geochemical data exist. The calculated water content was determined from both the 2.9 and 3.2 μm reflectances and was averaged, using the known SiO_2 concentration for each meteorite. Figure 7 shows the results. The measured water contents are derived from Hiroi et al. (2001) for Tagish Lake and from Jarosewich (1990) for the other 5 meteorites. The line in Fig. 7 represents where the points would lie if the calculated water contents were equal to the measured water contents. Note that this is not a best-fit line. The average difference between the water values calculated from the meteorite spectra and the known water values, weighted by the uncertainties in the spectral data, is $1.0\% \pm 1.7\%$. The unweighted average difference is $1.0\% \pm 2.7\%$. If only the 2.9 μm reflectance is used to determine the water content, the mean difference is smaller, though with larger uncertainties: $0.064\% \pm 2.2\%$ (unweighted) or $0.33\% \pm 2.5\%$ (weighted).

Note that all of these meteorites, except for Tagish Lake, were used by Sato et al. (1997) in finding the original correlations in their work. However, the spectra used in our test are from different sources (Hiroi et al. 1996, 2001). We also note that the reflectance ratios in this work use 2.50 μm rather than 2.53 μm as used by Sato et al. (1997). This is because 2.53 μm is a somewhat more difficult wavelength to observe from the ground. Because the reflectances of the target objects should not be changing appreciably between 2.50 and 2.53 μm , we expect the uncertainties introduced by this change to be negligible. Indeed, the fact that the meteorite data matches the known water values so closely is evidence of this.

We also include in Fig. 7 the results if we assume the meteorites have a weight percentage of 30% SiO_2 , as we do with the asteroids. As can be seen, for most of the meteorites

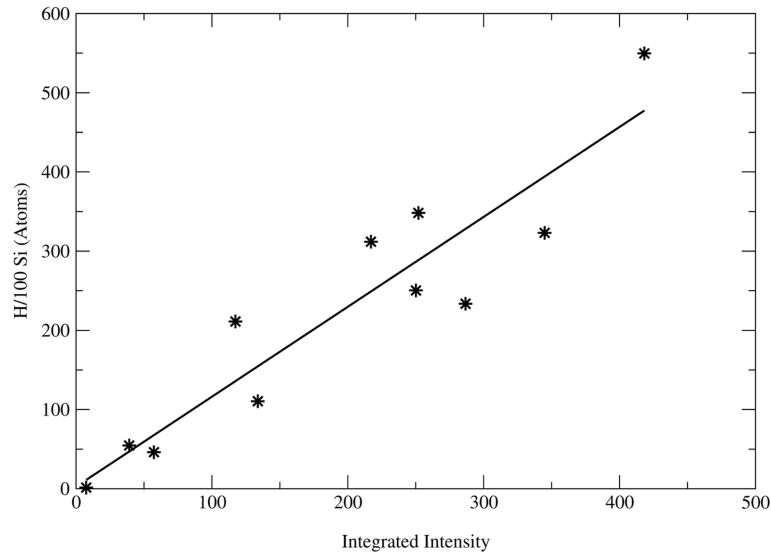


Fig. 5. Correlation between the integrated intensity and H/Si ratio in carbonaceous chondrites. Using a digitized version of Fig. 4 from Miyamoto and Zolensky (1994), we regenerated the linear correlation they reported for the integrated intensity of the 3 μm band for carbonaceous chondrite powders and their H/Si ratios and obtained the following relation: $\text{H}/100 \text{ Si} = 2.62935 + 1.13558 \times \text{integrated intensity}$. The equation for this best-fit line was combined with the equation for the best-fit line in the following figure to give Equations 1 and 2. The integrated intensity is in units of cm^{-1} .

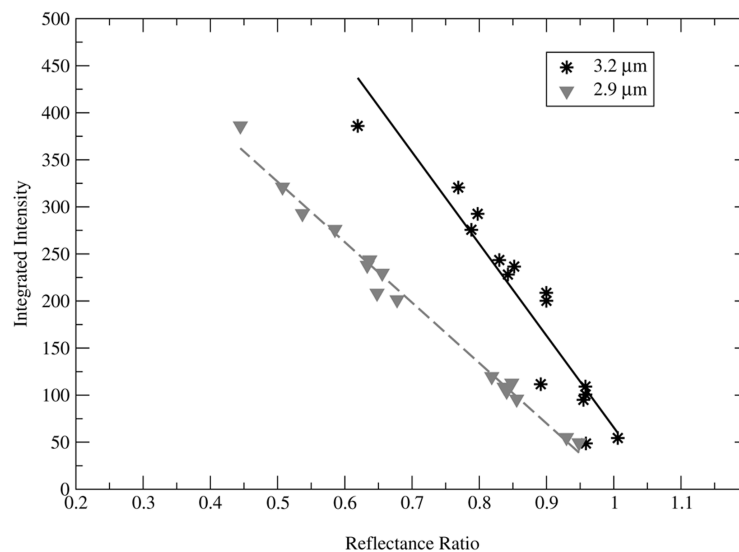


Fig. 6. Correlation between reflectance ratios in the 3 μm region and integrated intensity in carbonaceous chondrites. Using digitized versions of Fig. 3 from Sato et al. (1997), we regenerated the linear correlation they reported for 2.9 μm and 3.2 μm reflectance ratios, resulting in the following relations: $\text{integrated intensity} = 647.63 - 641.90 R_{2.9}/R_{2.53}$ and $\text{integrated intensity} = 1040.82 - 975.21 R_{3.2}/R_{2.53}$. The equations for these best fit lines were combined with the equation for the best-fit line in Fig. 5 to give Equations 1 and 2. The integrated intensity is in units of cm^{-1} .

the change is relatively small, but for Orgueil, which has a large amount of water but a small bulk SiO_2 content, the effect is relatively large.

Results for Asteroids

The H/Si ratios calculated for the asteroids using both the 2.9 μm and 3.2 μm ratios is shown in Fig. 8. Although

the H/Si values derived from the 3.2 μm data are shown, we will only discuss the 2.9 μm derived values. This is because uncertainties in thermal corrections lead to additional uncertainties in the H/Si ratio of roughly 0.5 in the 3.2 μm -derived data, which are not reflected in the figure. These same uncertainties only amount to ~ 0.1 or less in the 2.9 μm -derived H/Si values. The meteorite zones are based on data from falls in Jarosewich (1990), with estimated bounds.

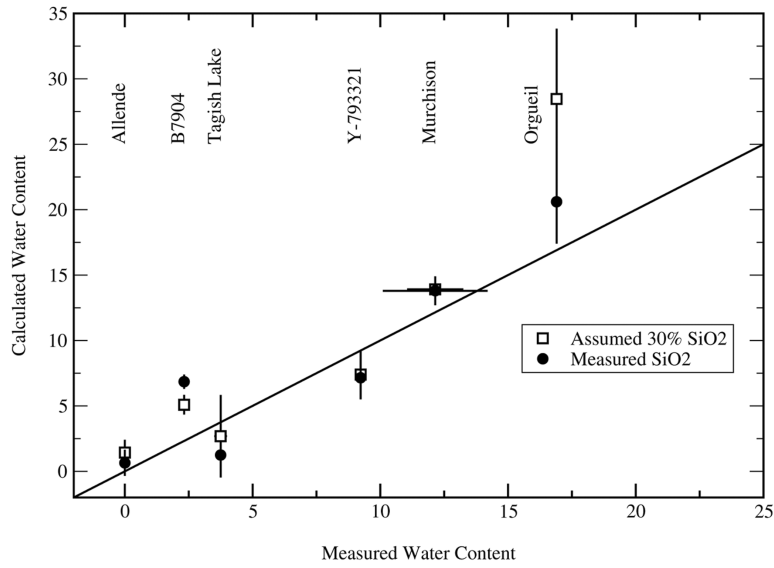


Fig. 7. Using Equations 1 and 2, we determined the equivalent water content for 6 carbonaceous chondrites for which we have both geochemical data and reflectance spectra. The solid line is where predicted equals known values and represents where the points should fall given perfect data and a perfect method. It is not a best-fit line. The closed symbols use the known SiO₂ values from Jarosewich (1990); the open symbols assume a SiO₂ concentration of 30%.

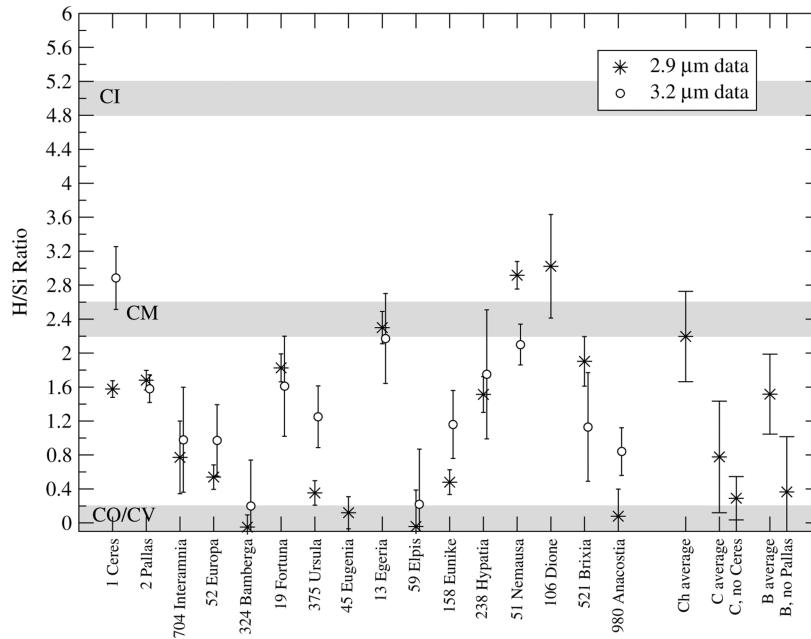


Fig. 8. The calculated H/Si ratios for C-class and related asteroids (using Bus taxonomy). The Ch asteroids, as a group, have water contents consistent with the CM chondrites. The individual asteroids seem to form 2 groups, with the more hydrogen-rich group itself splitting into 2 groups. None of the target asteroids are consistent with CI H/Si ratios. The class-average H/Si ratios were calculated using the 2.9 μm reflectance only, and the asteroids are in order of decreasing size. For 45 Eugenia and 106 Dione, the 2.9 μm data are only shown because the size of the uncertainties in their 3.2 μm data makes their inclusion of limited use.

The asteroids fall into 2 main groups, with the first group perhaps really representing 2 subgroups: 1a) H/Si >2 (51 Nemausa, 13 Egeria, 106 Dione). These asteroids have H/Si ratios similar to or slightly greater than the CM meteorites; 1b) H/Si ~1.6 (5 asteroids). This H/Si ratio is roughly 2/3 that of the CM value. This group may be combined with the

first group; 2) H/Si <0.8 (8 asteroids). This group includes both asteroids that are anhydrous within uncertainties and those which have a small amount of hydrated minerals. The CV and CO chondrites have similar amounts (or lack of) hydrated minerals, but these values are not diagnostic for these meteorite groups; metamorphosed carbonaceous

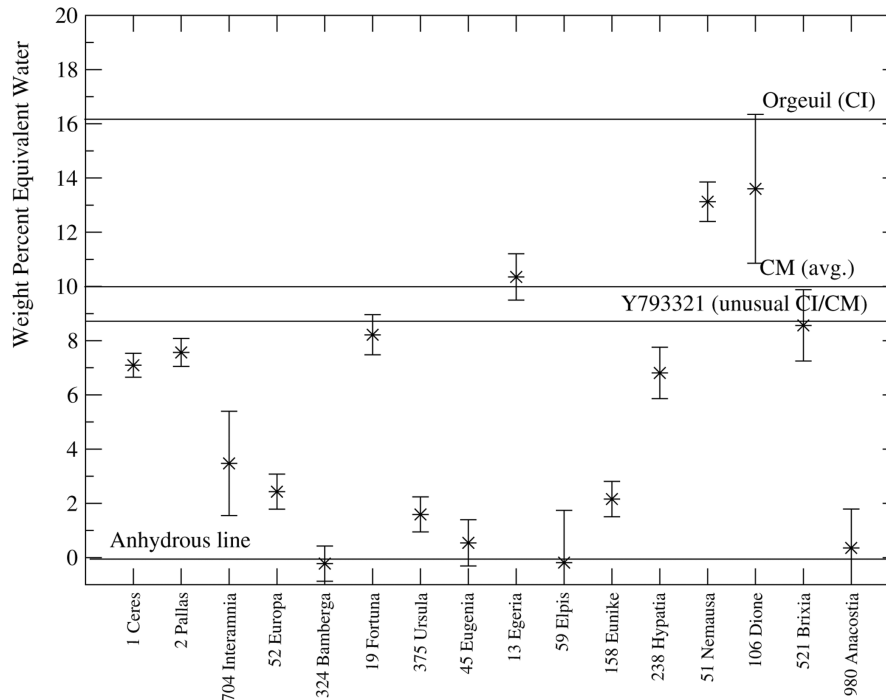


Fig. 9. The calculated water contents for C-class and related asteroids. These values were calculated assuming a CM-like SiO_2 weight percentage and using the H/Si ratio from the previous figure. Because the H/Si ratio is lower than CM values for most of these objects, the calculated water contents are also lower than CM values. On this figure, values for specific meteorites rather than shaded ranges are shown.

chondrites of other groups also contain little or no hydrated minerals.

Figure 8 also shows the averages for different Bus classes. Taken as a whole, the Ch asteroids have H/Si ratios consistent with CM meteorites. The C and B classes have ratios that are much lower, particularly if Ceres and Pallas are excluded. Ceres is an unusual asteroid in terms of its $3 \mu\text{m}$ spectrum, and its exclusion from the C asteroid average is justifiable on those grounds. Excluding Pallas from the B asteroid average is more arbitrary. At this point, with only 3 B asteroids surveyed, whether Pallas is truly unusual compared to its classmates or whether the B class spans a wide range of H/Si ratios is unclear.

DISCUSSION

Ceres and Ursula

Figure 10 shows the spectra of 1 Ceres and 375 Ursula (with a linear continuum removed), the 2 asteroids in this sample that do not follow the carbonaceous chondrite trend in Fig. 4. Ceres was thought to be unique among low-albedo asteroids in its unusual band shape. The interpretation of this shape as being due to ammoniated silicates by King et al. (1992) suggests aqueous alteration by a fluid containing NH_4^+ and constrains the temperatures experienced by Ceres' surface to 400 K or less (Lewis and Prinn 1984; Chourabi and Fripiat 1981). Ceres' current maximum surface temperature is

~235 K (Tedesco et al. 1992; Saint-Pe et al. 1993). The alternate interpretation for Ceres' surface, that of water frosts, is only possible at very high latitudes at Ceres' surface temperatures (Fanale and Salvail 1989).

The spectrum of 375 Ursula is similar to that of Ceres, though the wavelengths of band minima are not identical. Ursula is farther from the sun, though its lower albedo, compared to Ceres, will raise its temperature. These competing effects result in a surface temperature only ~10 K cooler than that of Ceres. This difference in temperature is unlikely to make water ice stable over large portions of Ursula's surface. A low-temperature ammoniated phyllosilicate interpretation is preferred for this reason, though this may not be the only possibility. Higher-albedo asteroids with $3 \mu\text{m}$ features (e.g., 44 Nysa, 92 Undina, 21 Lutetia) have been found to have rounded bands that are, at least superficially, like those on Ceres and Ursula. We note that Ursula is classified as Xc in the Bus taxonomy, which is the same class as 44 Nysa, though the albedos are vastly different for these 2 asteroids (0.032 for Ursula, 0.546 for Nysa [Millis et al. 1984; Tedesco et al. 1992]). At this point, how common low-albedo asteroids with rounded $3 \mu\text{m}$ bands are is unclear, though Ceres and Ursula are unlikely to be the only 2.

G-Class Asteroids

In the Tholen (1984) taxonomy, the G class is a subclass related to the C, F, and B classes. The Bus and Binzel (2002)

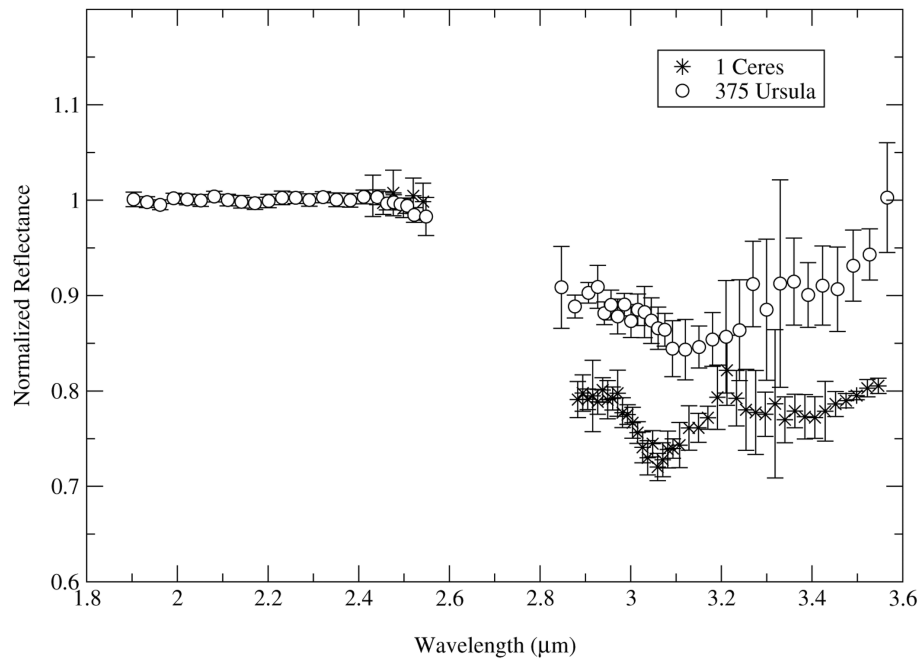


Fig. 10. Spectra of 1 Ceres and 375 Ursula. These 2 objects fall off of the meteorite trend shown in Fig. 5. Ceres is well-known to have an unusual band shape at 3 μm and has a surface interpreted as either containing a water ice frost (Lebofsky 1981) or ammoniated phyllosilicates (King et al. 1992). The Ursula spectrum, shown with a linear continuum removed to facilitate comparison, shows a similar spectrum. This suggests that Ceres' surface mineralogy is not unique. It also favors the ammoniated phyllosilicate interpretation, since water frost was only marginally stable on Ceres (Fanale and Salvail 1989).

taxonomy does not include a G class. Vilas (1994) found the G-class asteroids to be the most hydrated of the CBGF clan, based on the presence on most of these asteroids of the 0.7 μm band correlated with hydrated minerals. Burbine (1998) proposed that the G-class asteroids were analogues for the CM chondrites based upon their 0.3–2.5 μm spectra (particularly their 0.7 μm band), as well as dynamical arguments. Four of the asteroids in our sample are G asteroids: 1 Ceres, 13 Egeria, 19 Fortuna, and 106 Dione. Ceres is unusual for several reasons, as mentioned above, and can be discounted. Interestingly, Egeria and Dione are 2 of the 3 asteroids with water contents consistent with the CM average within observational uncertainties, and Fortuna is also in the high-water group. This supports the hypothesis of Burbine (1998).

Where Are the CI Parents?

The lack of parent bodies with CI-like H/Si ratios is striking. One possibility is that our sample size is still relatively small, and we have not come across any CI parent bodies yet. Related to that is the possibility that CI parent bodies are not very common in the asteroid belt, so we will need to observe many more objects before finding one. A third possibility is that CI material is found mixed with less-hydrated or anhydrous material on the surface of its parent body(ies), lowering the apparent H/Si ratio to CM levels or below. Given the pervasiveness of aqueous alteration in CI

meteorites, however, combined with their brecciated nature, we do not suspect that this is the case. Also, conceivably, regolith processes have dehydrated CI surfaces to appear more like CM-like surfaces in terms of H/Si ratio. We discuss this below. Finally, given the fragility of CI material, the CI meteorites possibly come from objects too small (and thus too faint) to be observed at 3 μm with current telescopes and instruments. Given these options, we believe the likeliest is a combination of the first, second, and last: that CI material is relatively rare at large asteroidal sizes and that our sample size is too small to be certain of seeing one.

Regolith Processes and Hydrated Minerals

There are 2 ways that regolith processes could plausibly change the 3 μm spectra of hydrated bodies. First, vapor-deposited nanophase iron (npFe) could alter spectral properties of surfaces without necessarily changing their compositions. This process, often called “space weathering,” is observed in the visible and near-IR spectra of lunar soils and is also thought to be present in the visible and near-IR spectra of S asteroids (Sasaki et al. 2001; Pieters et al. 2000). The effect lessens as wavelength increases and in low-albedo ($p_v \sim 0.1$ or less) objects, which suggests that this will not be an important concern here. We note that experiments on npFe deposition in carbonaceous chondrites are currently underway.

A second possibility is that impacts into the surface of a hydrated asteroid could devolatilize and dehydrate the

regolith. This would presumably lead to a surface with little or no obvious 3 μm band covering a hydrated interior. In this case, 3 μm observations would only provide a lower limit to band depth and a lower limit to water content, though the observations would accurately depict the surface mineralogy.

The observations presented here directly touch on the question of spectral alteration in the 3 μm region and allow us to quantitatively estimate the relative rate at which any putative dehydration may occur. If dehydration were to occur quickly relative to regolith turnover timescales, we would expect most of the asteroids to have H/Si ratios near zero, with only rare instances of H/Si values higher than that. This is not the case in our sample. If dehydration were occurring on the same timescale as regolith turnover, we would expect to see objects throughout the range of H/Si ratios, with perhaps more in the middle. This is arguably the case here, though our sample size is too small to make a strong case either way. Finally, if dehydration is very slow relative to regolith turnover, we would expect objects to remain near their bulk H/Si values. Again, this is arguably the case here. The CM-like H/Si ratios for the G-class asteroids suggest that the proposed G-CM link can be interpreted with no need to consider regolith effects and that dehydration is not important, at least for that group.

Hiroi et al. (1996) suggested that large C-class (and the related B-, G-, and F-class) asteroids were thermally metamorphosed early in solar system history, based on the relative strengths of their 0.7 μm and 3 μm bands. The data presented here do not explicitly address these findings, but do

provide an additional 11 asteroids with which to test their model. We recalculated the 0.7 μm band depth for 14 of our target asteroids using the ECAS data of Zellner et al. (1985) and the formula included in Vilas (1994) and compared it to the 2.9 μm band depth in Table 3. This is shown in Fig. 11. The asteroids 324 Bamberga and 375 Ursula do not have ECAS data at the necessary wavelengths and were omitted. Figure 11 shows a correlation between the 2 band depths, although it is not a perfect one. This is consistent with the idea that thermal effects may have destroyed phyllosilicates and weakened the 3 μm and 0.7 μm bands in tandem. However, this is not a unique interpretation, and a number of large asteroids like 2 Pallas with a strong 3 μm band but little or no 0.7 μm absorption need an alternate explanation.

FUTURE WORK

At this point, reflectances at 2.5 and 2.9 (and/or 3.2) μm are necessary to determine H/Si ratios for C-class asteroids directly from reflectance spectra using the relations outlined above. The majority of asteroid data collected thus far for these objects in the 3 μm region is spectrophotometric rather than spectroscopic, however (Lebofsky 1980; Feierberg et al. 1985; Britt et al. 1994), and reflectances at 2.9 and 3.2 μm are not available. However, because the 3 μm band for most hydrated asteroids has a simple, linear slope through 2.9 and 3.2 μm out to the continuum, we should be able to recalculate Equations 1 and 2 for other wavelengths inside the 3 μm band. This would dramatically increase our sample size of usable data.

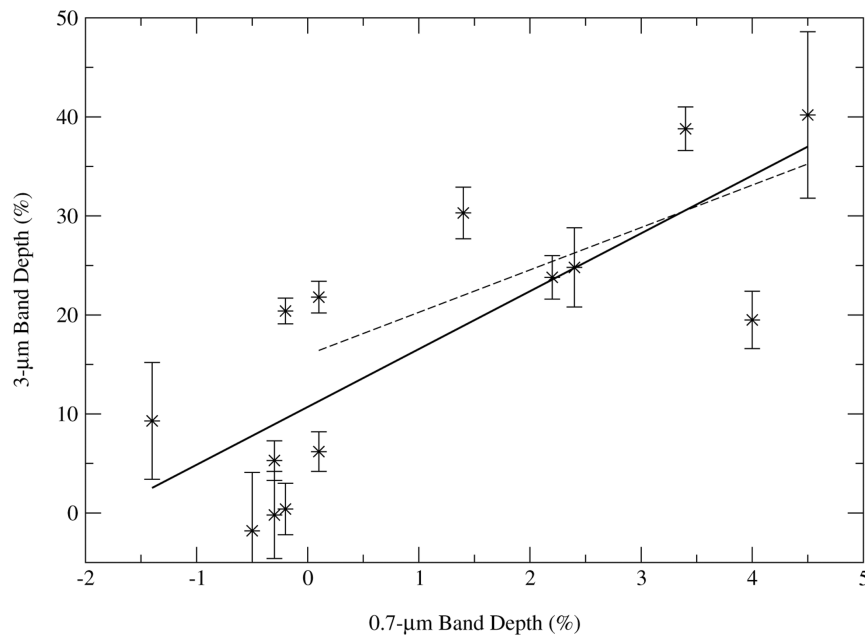


Fig. 11. Correlation between the 0.7 μm band and the 3 μm band depths. The 0.7 μm band depth was determined using ECAS data (Zellner 1985) and the test of Vilas (1994). The 3 μm band depths are from this work. The solid line shows the best-fit line including all of the points. The dashed line includes only points that have positive values for band depth. A correlation between these 2 values exists in both cases, with a correlation coefficient of 0.783 when all of the points are included and 0.651 with the smaller set of points.

The discovery of a 3 μm band on M-, S-, and E-class asteroids (Jones et al. 1990; Rivkin et al. 1995, 2000, 2001) potentially allows remote determination of H/Si for these bodies as well. However, their higher albedos make it uncertain whether carbonaceous chondrite powders are sufficiently analogous to their surfaces. Clark (1983) showed that the 3 μm band in montmorillonite decreased in depth with increasing amounts of carbon mixed in. With over 90% of the spectrally opaque carbon mixed in, the 3 μm band decreased in strength by 50%. As an initial guess, we might be able to simply divide the band depths by 2 on these high-albedo objects to simulate mixing in 90% opaques and creating a carbonaceous chondrite-like albedo. A rigorous assessment of this technique will be required to determine the feasibility of this approach for generating H/Si values.

CONCLUSIONS

We have observed 16 low-albedo objects in the 3 μm region from UKIRT from 1996–2000. Using relations first derived for meteorites by Miyamoto and Zolensky (1994) and Sato et al. (1997), we have determined the hydrogen to silicon ratios for these bodies, which divide into 2 groups. Some of the targets are consistent with CM meteorite values for H/Si, but none are consistent with CI meteorites. We believe this suggests that CI parent bodies are relatively uncommon. We found 375 Ursula to have a 3 μm band shape reminiscent of 1 Ceres, suggesting that the former asteroid may have a surface containing ammoniated silicates, as has been proposed for Ceres.

Band depths at 3 μm and 0.7 μm appear correlated, though individual objects may vary. Future work includes adapting the H/Si relations to allow for archival data to be analyzed and attempting to expand our analysis to asteroids of types other than carbonaceous chondrite-like asteroids.

Acknowledgments—This work was supported by NASA grants NAG5–10604 and NAG5–11617. The United Kingdom Infrared Telescope is operated by the Joint Astronomy Centre on behalf of the U.K. Particle Physics and Astronomy Council. Mahalo nui loa to the telescope operators at UKIRT and the support crew on Mauna Kea. The majority of the observing and much of the work in this paper was conducted by A. S. Rivkin while he was at the University of Arizona. We also extend our gratitude to the people of Hawaiian descent, who have allowed us to visit their sacred mountain of Mauna Kea to conduct our research.

Editorial Handling—Dr. Anita Cochran

REFERENCES

- Britt D. T., Rivkin A. S., Howell E. S., and Lebofsky L. A. 1994. Observations of “dry” C-class asteroids. *Bulletin of the American Astronomical Society* 26:1175.
- Burbine T. H. 1998. Could G-class asteroids be the parent bodies of the CM chondrites? *Meteoritics & Planetary Science* 33:253–258.
- Burbine T. H., Gaffey M. J., and Bell J. F. 1992. S-asteroids 387 Aquitania and 908 Anacostia: Possible fragments of the breakup of a spinel-bearing parent body with CO3/CV3 affinities. *Meteoritics* 27:424–434.
- Bus S. J. and Binzel R. P. 2002. Phase II of the Small Main-Belt Asteroid Spectroscopic Survey: A feature-based taxonomy. *Icarus* 158:146–177.
- Chourabi B. and Fripiat J. J. 1981. Determination of tetrahedral substitutions and interlayer surface heterogeneity from vibrational spectra of ammonium in smectites. *Clays and Clay Minerals* 29:260–268.
- Clark R. N. 1983. Spectral properties of mixtures of montmorillonite and dark carbon grains: Implications for remote sensing minerals containing chemically and physically adsorbed water. *Journal of Geophysical Research* 88:10635–10644.
- Cruikshank D. P., Geballe T. R., Owen T. C., Dalle Ore C. M., Roush T. L., Brown R. H., and Lewis J. H. 2002. Search for the 3.4 μm C-H spectral bands on low-albedo asteroids. *Icarus* 156:434–441.
- Delsemme A. H. 2000. 1999 Kuiper Prize lecture. *Icarus* 146:313–325.
- DuFresne E. R. and Anders E. 1962. On the chemical evolution of the carbonaceous chondrites. *Geochimica et Cosmochimica Acta* 26:1084–1114.
- Emery J. P. 2002. Constraints on the surface composition of Trojan asteroids from near infrared (0.8–4.0 μm) spectroscopy and spectral modeling. Ph.D. dissertation, University of Arizona, Tucson, Arizona, USA.
- Fanale F. P. and Salvail J. R. 1989. The water regime of asteroid (1) Ceres. *Icarus* 82:97–110.
- Feierberg M. A., Lebofsky L. A., and Tholen D. 1985. The nature of C-class asteroids from 3 μm spectrophotometry. *Icarus* 63:183–191.
- Gaffey M. J., Bell J. F., and Cruikshank D. P. 1989. Reflectance spectroscopy and asteroid surface mineralogy. In *Asteroids II*, edited by Binzel R., Gehrels T., and Matthews M. S. Tucson: University of Arizona Press. pp. 98–127.
- Harris A. W. 1998. A thermal model for near-earth asteroids. *Icarus* 131:291–301.
- Hiroi T., Zolensky M. E., and Pieters C. M. 2001. The Tagish Lake meteorite: A possible sample for a D-type asteroid. *Science* 293:2234–2236.
- Hiroi T., Zolensky M. E., Pieters C. M., and Lipschutz M. E. 1996. Thermal metamorphism of the C, G, B, and F asteroids seen from the 0.7 μm , 3 μm , and UV absorption strengths in comparison with carbonaceous chondrites. *Meteoritics & Planetary Science* 31:321–327.
- Hörz F., Grieve R., Heiken G., Spudis P., and Binder A. 1991. Lunar surface processes. In *Lunar sourcebook: A user's guide to the Moon*, edited by Heiken G. H., Vaniman D. T., and French B. M. Cambridge: Cambridge University Press. pp. 61–120.
- Howell E. S., Rivkin A. S., and Vilas F. 2001. Uneven distribution of aqueously altered minerals on asteroids. In *Asteroids 2001: From Piazzi to the third millennium*. pp. 62.
- Jarosewich E. 1990. Chemical analyses of meteorites: A compilation of stony and iron meteorite analyses. *Meteoritics* 25:323–337.
- Jones T. D. 1988. An infrared reflectance study of water in outer belt asteroids: Clues to composition and origin. Ph.D. dissertation, University of Arizona, Tucson, Arizona, USA.
- Jones T. D., Lebofsky L. A., Lewis J. S., and Marley M. S. 1990. The composition and origin of the C, P, and D asteroids: Water as a tracer of thermal evolution in the outer belt. *Icarus* 88:172–192.

- King T. V. V., Clark R. N., Calvin W. M., Sherman D. M., and Brown R. H. 1992. Evidence for ammonium-bearing minerals on Ceres. *Science* 255:1551–1553.
- Koornneef J. 1983. Near-infrared photometry. II: Intrinsic colours and absolute calibration from one to five microns. *Astronomy and Astrophysics* 128:84–93.
- Larson H. P., Feierberg M. A., and Lebofsky L. A. 1983. The composition of 2 Pallas and its relation to primitive meteorites. *Icarus* 56:398–408.
- Lebofsky L. A. 1978. Asteroid 1 Ceres: Evidence for water of hydration. *Monthly Notices of the Royal Astronomical Society* 182:17–21.
- Lebofsky L. A. 1980. Infrared reflectance spectra of asteroids: A search for water of hydration. *The Astronomical Journal* 85:573–585.
- Lebofsky L. A., Feierberg M. A., Tokunaga A. T., Larson H. P., and Johnson J. R. 1981. The 1.7- to 4.2-micron spectrum of asteroid 1 Ceres: Evidence for structural water in clay minerals. *Icarus* 48:453–459.
- Lebofsky L. A. and Spencer J. R. 1989. Radiometry and thermal modeling of asteroids. In *Asteroids II*, edited by Binzel R., Gehrels T., and Matthews M. S. Tucson: University of Arizona Press. pp. 128–147.
- Lebofsky L. A., Sykes M. V., Tedesco E. F., Veeder G. J., Matson D. L., Brown R. H., Gradie J. C., Feierberg M. A., and Rudy R. J. 1986. A refined “standard” thermal model for asteroids based on observations of 1 Ceres and 2 Pallas. *Icarus* 68:239–251.
- Lewis J. S., McKay D. S., and Clark B. C. 1993. Using resources from near-Earth space. In *Resources of near-Earth space*, edited by Lewis J. S., Matthews M. S., and Guerrieri M. L. Tucson: University of Arizona Press. pp. 3–14.
- Lewis J. S. and Prinn R. G. 1984. *Planets and their atmospheres: Origin and evolution*. Orlando: Academic Press.
- Millis R. L., Wasserman L. H., Bowell E., Franz O. G., Klemola A., and Dunham D. W. 1984. The diameter of 375 URSULA from its occultation of AG + 395#5 303. *The Astronomical Journal* 89: 592–596.
- Miyamoto M. and Zolensky M. E. 1994. Infrared diffuse reflectance spectra of carbonaceous chondrites: Amount of hydrous minerals. *Meteoritics* 29:849–853.
- Morbidelli A., Chambers J., Lunine J. I., Petit J. M., Robert F., Valsecchi G. B., and Cyr K. E. 2000. Source regions and time scales for the delivery of water to earth. *Meteoritics & Planetary Science* 35:1309–1320.
- Mountain C. M., Robertson D. J., Lee T. J., and Wade R. 1990. An advanced cooled grating spectrometer for UKIRT. In *Instrumentation in astronomy VII*. Bellingham: Society of Photo-Optical Instrumentation Engineers. pp. 25–33.
- Pieters C., Taylor L. A., Noble S. K., Keller L. P., Hapke B., Morris R. V., Allen C. C., McKay D. S., and Wentworth S. 2000. Space weathering on airless bodies: Resolving a mystery with lunar samples. *Meteoritics & Planetary Science* 35:1101–1107.
- Rivkin A. S., Davies J. K., Clark B. E., Trilling D. E., and Brown R. H. 2001. Aqueous alteration on S Asteroid 6 Hebe? (abstract #1723). 32nd Lunar and Planetary Science Conference.
- Rivkin A. S., Howell E. S., Britt D. T., Lebofsky L. A., Nolan M. C., and Branston D. D. 1995. 3 μm spectrophotometric survey of M and E-class asteroids. *Icarus* 117:90–100.
- Rivkin A. S., Lebofsky L. A., Clark B. E., Howell E. S., and Britt D. T. 2000. The nature of M-class asteroids in the 3 μm region. *Icarus* 145:351–368.
- Saint-Pe O., Combes M., and Rigaut F. 1993. Ceres surface properties by high-resolution imaging from earth. *Icarus* 105: 271–281.
- Salisbury J. W., Walter L. S., Vergo N., and D’Aria D. M. 1991. *Infrared (2.1–25 μm) spectra of minerals*. Baltimore: Johns Hopkins University Press.
- Sasaki S., Nakamura K., Hamabe Y., Kurahashi E., and Hiroi T. 2001. Production of iron nanoparticles by laser irradiation in a simulation of lunar-like space weathering. *Nature* 410:555–557.
- Sato K., Miyamoto M., and Zolensky M. E. 1997. Absorption bands near three micrometers in diffuse reflectance spectra of carbonaceous chondrites: Comparison with asteroids. *Meteoritics & Planetary Science* 32:503–507.
- Storrs A., Weiss B., Zellner B., Bursleson W., Sichertiu R., Wells E., Kowal C., and Tholen D. 1999. Imaging observations of asteroids with Hubble Space Telescope. *Icarus* 137:260–268.
- Tedesco E. F., Veeder G. J., Fowler J. W., and Chillemi J. R. 1992. *The IRAS Minor Planet Survey Data Base* (digital data). Greenbelt: National Space Science Data Center.
- Tholen D. J. 1984. Asteroid taxonomy from cluster analysis of photometry. Ph.D. dissertation, University of Arizona, Tucson, Arizona, USA.
- Vilas F. 1994. A cheaper, faster, better way to detect water of hydration on solar system bodies. *Icarus* 111:456–467.
- Zellner B., Tholen D. J., and Tedesco E. F. 1985. The eight-color asteroid survey: Results for 589 minor planets. *Icarus* 61:355–416.
- Zolensky M. E., Krot A. N., and Scott E. R. D., editors. 1997. Workshop on parent-body and nebular modifications of chondritic materials. Lunar and Planetary Institute. LPI Technical Report 97–02, Part 1.